

Progress in the development of critical-angle transmission gratings

Ralf K. Heilmann, Alex R. Brucoleri, Pran Mukherjee, and Mark L. Schattenburg,

Space Nanotechnology Laboratory, MIT Kavli Institute for Astrophysics and Space Research,
Massachusetts Institute of Technology, Cambridge, Massachusetts 02139, USA

ABSTRACT

Recently developed Critical-Angle Transmission (CAT) grating technology - in combination with x-ray CCD cameras and large collecting-area focusing optics - will enable a new generation of soft x-ray spectrometers with unprecedented resolving power and effective area and with at least an order of magnitude improvement in figures-of-merit for emission and absorption line detection. This technology will be essential to address a number of high-priority questions identified in the Astro2010 Decadal Survey “New Worlds New Horizons” and open the door to a new discovery space. CAT gratings combine the advantages of soft x-ray transmission gratings (low mass, relaxed figure and alignment tolerances, transparent at high energies) and blazed reflection gratings (high broad band diffraction efficiency, utilization of higher diffraction orders to increase resolving power). We report on progress in the fabrication of large-area ($31 \times 31 \text{ mm}^2$) free-standing gratings with two levels of low-blockage support structures using highly anisotropic deep reactive-ion etching.

Keywords: x-ray optics, critical-angle transmission grating, x-ray spectroscopy, blazed transmission grating, soft x-ray, silicon-on-insulator, deep reactive-ion etching

1. INTRODUCTION

Grating spectroscopy of celestial point sources with high resolving power and large effective area is essential for the study of the large scale structure of the universe and its growth and interaction with supermassive black holes, and the kinematics of galactic outflows, hot gas in galactic halos, and disc accretion, including the growth of smaller black holes. The same technique can look for missing baryons in the intergalactic medium and inside of galaxies. Existing x-ray spectrographs (Chandra High Energy Transmission Grating Spectrometer (HETGS)¹ and XMM-Newton Reflection Grating Spectrometer (RGS),² both launched in 1999) lack the effective area and resolving power to reveal more than tantalizing hints of relevant observations on these subjects. Due to their transmission geometry the Chandra transmission gratings have relaxed alignment and flatness tolerances and extremely low mass, but they also have low diffraction efficiency in the soft x-ray band of interest ($\sim 0.3 - 1.5 \text{ keV}$) for the above subjects of inquiry. Most photons diffract in first order, which limits spectral resolving power. The blazed reflection gratings of the RGS utilize higher orders and are more efficient at longer wavelengths, but the grazing incidence reflection geometry makes them very alignment and figure sensitive, as well as much more massive.

Critical-angle transmission (CAT) gratings are free-standing transmission gratings with ultra-high aspect-ratio grating bars that combine the advantages of past-generation transmission and blazed reflection gratings and can be described as blazed transmission gratings.³⁻⁶ In combination with large collecting area optics (5 – 10 arcsec point-spread function (PSF) half power diameter (HPD)) and order-sorting x-ray CCD cameras, CAT gratings are a natural match for high-efficiency, large resolving power soft x-ray spectroscopy with order-of-magnitude improved performance at minimum cost and complexity.⁷⁻⁹ For silicon CAT gratings the misalignment-tolerant transmission geometry only requires temperature control a factor 5 – 10 more relaxed than typical segmented grazing-incidence Wolter-type optics; this often can be achieved passively simply through the proximity of gratings to the actively temperature-controlled optics.⁹ This reduces mass and power in addition to the already low mass of the gratings themselves.

Further author information: Send correspondence to R.K.H. E-mail: ralf@space.mit.edu, URL: <http://snl.mit.edu/home/ralf>

We have fabricated a number of CAT grating prototypes in the past¹⁰⁻¹² and demonstrated good agreement in soft x-ray diffraction efficiency (80 – 100% of theoretical predictions over most of the relevant band).^{3-5,8} Our current focus is on the fabrication of large-area gratings with minimal integrated support structures.

In the following we briefly review post-IXO (International X-ray Observatory) CAT grating-based mission concepts and parameters for CAT grating design and fabrication. We then present our recent progress in fabrication of large-area gratings, followed by discussion and summary.

2. NEW CAT-GRATING-BASED MISSION CONCEPTS

The Astro2010 Decadal Survey “New Worlds New Horizons” (NWNH)¹³ endorsed IXO¹⁴ as “a versatile, large-area, high-spectral-resolution X-ray telescope that will make great advances on broad fronts ranging from characterization of black holes to elucidation of cosmology and the life cycles of matter and energy in the cosmos.” As part of its science case IXO carried a large-area ($> 1000 \text{ cm}^2$), high resolving power ($R = \lambda/\Delta\lambda > 3000$) x-ray grating spectrometer (XGS).^{9,15} However, NWNH did not rank IXO as the highest priority for launch by 2020. Together with budgetary constraints and a mismatch between NASA and ESA schedules IXO was cancelled, and a smaller ESA-only Advanced Telescope for High Energy Astrophysics (ATHENA)¹⁶ concept was submitted to the ESA Cosmic Visions planning process. Subsequently, ATHENA was not selected for ESA’s next L-class mission launch. On the US side a (scaled down from IXO) mission concept named AXSIO (Advanced X-ray Spectroscopic Imaging Observatory)^{17,18} was developed with NWNH recommendations in mind, only carrying a microcalorimeter and a CAT grating spectrometer.

Last fall NASA asked the x-ray astronomy community for “information that can be used to develop concepts that meet some or all of the scientific objectives of the International X-ray Observatory.” In response to this Request For Information (RFI) two more mission concepts with CAT grating spectrometers were submitted in addition to AXSIO: A stand-alone grating spectrometer mission named AEGIS (Astrophysics Experiment for Grating and Imaging Spectroscopy)¹⁹⁻²¹ and the Square Meter, Arcsecond Resolution X-ray Telescope (SMART-X).^{22,23} A workshop based on all RFI responses was held, and a Community Science Team (CST) was appointed to define a small number of notional mission concepts in the \$300M to \$2B cost range. Mission Design Lab (MDL) runs were performed for four mission concepts. Due to the limited resources available, a single MDL run was performed for a “gratings-only” mission (Notional X-ray Grating Spectrometer - NXGS)²¹ similar in spirit to AEGIS or WHIMex,¹⁵ a reflection-grating-based RFI response. In order to avoid preclusion of either grating-based spectrometer design, a compromise (“worst case”) envelope was defined that could accommodate both designs. Unavoidably, this led to a design that was not optimized for either approach. Nevertheless the NXGS mission concept resulted in the lowest cost estimate out of the four MDL runs at $\sim \$600\text{-}700 \text{ M}$.

We believe that a grating spectrometry mission based on the AEGIS concept (which was conceived in less than six weeks and is not fully optimized either) is more representative of the cost vs. performance relationship than the NXGS. At $< \$800 \text{ M}$ it provides twice the effective area and the same resolving power as the NXGS. For a baseline three-year mission AEGIS will accumulate more than four times as much exposure as was planned for the IXO XGS. AEGIS will be 30-50 times more sensitive than any existing soft x-ray spectrometer (see Fig. 1). It employs a compact 4.4 m focal-length telescope with a 1.9 m diameter flight mirror assembly (FMA) of segmented glass optics (10 arcsec PSF (HPD)). The FMA is split azimuthally into twelve sectors, with a CAT grating array immediately downstream. The grating arrays behind each diametrically opposed sector pair diffract into a common CCD array, taking advantage of the narrowing of the PSF in the dispersion direction due to the sub-aperturing effect.²⁴ Thus AEGIS consists of six spectrometers with $R > 3500$ operating in parallel, adding up to $\sim 1400 \text{ cm}^2$ peak effective area. As an added benefit, if the six spectrographs are aligned to a common zeroth order, AEGIS will provide 10 arcsec imaging with an effective area $A > 900 \text{ cm}^2$ for $1.3 < E < 1.6 \text{ keV}$ and $A > 100 \text{ cm}^2$ for $E < 2 \text{ keV}$. Alternatively, one could offset the six spectrometers relative to each other and take advantage of the sub-aperturing effect by collecting six images with 2-3 arcsec PSF in one dimension. Thus by sampling six position angles, an image may be reconstructed with 2-3 arcsec resolution from a 10” optic.

Our ray-trace models for the IXO CATXGS, AXSIO, AEGIS, SMART-X, and NXGS show that a CAT grating-based spectrometer can be readily adapted to a range of telescope designs and provide $R > 3000$ even for optics with 10 arcsec PSF (HPD).

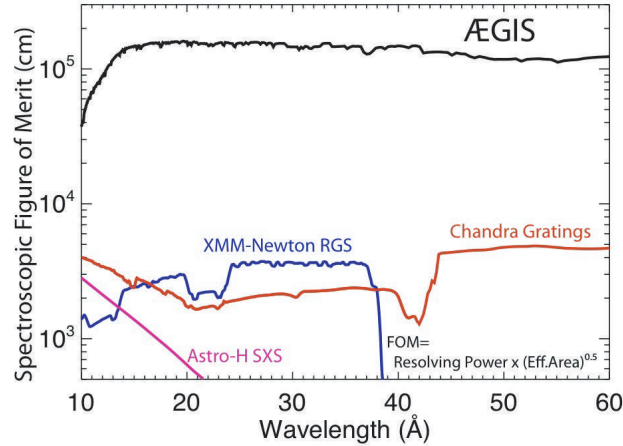


Figure 1. Figure of merit for the accuracy of line centroid (or velocity) measurements for AEGIS,¹⁹ the Chandra gratings, the XMM-Newton RGS, and the future Astro-H Soft X-ray Spectrometer (SXS).²⁵

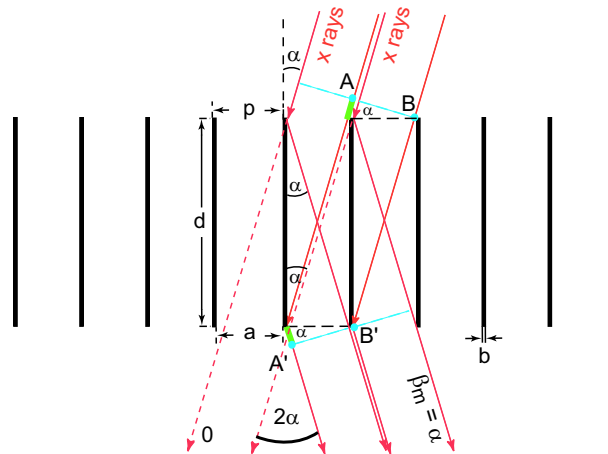


Figure 2. Schematic cross section through a CAT grating. The m^{th} diffraction order occurs at an angle β_m where the path length difference between AA' and BB' is $m\lambda$. Shown is the case where β_m coincides with the direction of specular reflection from the grating bar side walls ($\beta_m = \alpha$), i.e., blazing in the m^{th} order.

3. CAT GRATING PRINCIPLE

CAT gratings are blazed transmission gratings. In the geometrical optics approximation x rays are incident onto the nm-smooth side walls of thin, ultra-high aspect-ratio grating bars at an angle α below the critical angle for total external reflection, θ_c . In order for every x ray incident upon the space between grating bars to undergo exactly one reflection, the grating depth $d = a / \tan \alpha$, with a being the distance between two adjacent grating bars. Since θ_c is rather small for x rays (e.g. $\theta_c = 1.7^\circ$ for 1 keV photons reflecting off a silicon surface), the grating depth is much greater than the grating period $p = a + b$. The grating bar thickness b should be as small as possible to minimize absorption. The gratings should be free-standing for the same reason. For example, if $p = 200$ nm and $b = 40$ nm, then for $\alpha = 1.7^\circ$ we need $d = 5.39$ μm , which means the aspect ratio d/b for the grating bar cross section is ~ 135 .

We have previously fabricated small CAT grating prototypes with periods of 574^{3,4,10} and 200 nm^{4,5,8,9,11} with anisotropic wet etching of lithographically patterned <110> silicon-on-insulator (SOI) wafers in potassium hydroxide (KOH) solutions. We have achieved small grating bar duty cycles ($b/p < 20\%$), unprecedented grating bar aspect ratios (d/b up to 150), and smooth side walls. X-ray tests have shown that our grating prototypes perform at the level of 50-100% of theoretical predictions for ideal CAT gratings over a broad wavelength band.^{3,5}

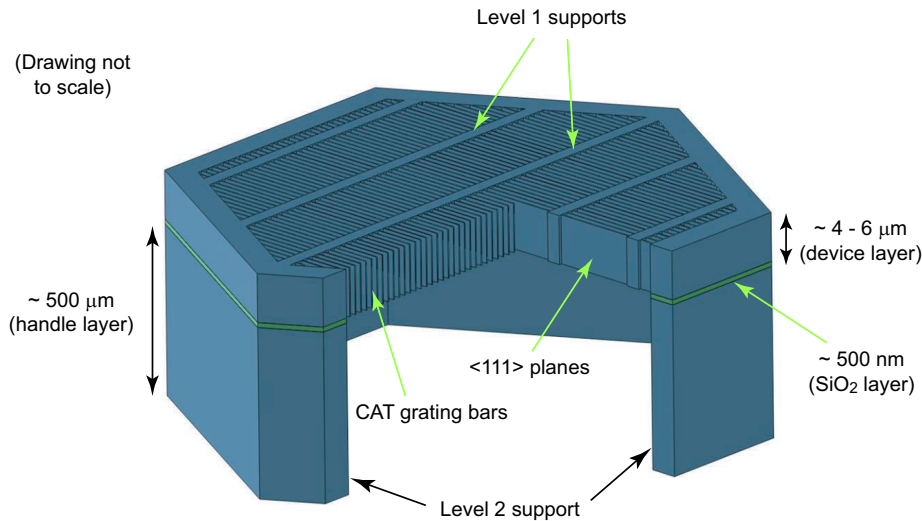


Figure 3. Schematic of a grating membrane “unit cell” (not to scale), formed by a single L2 support mesh hexagon. The L2 mesh is etched out of the SOI handle layer (back side). The device layer contains the fine-period CAT grating bars and in the perpendicular direction the coarse, low duty cycle integrated L1 support mesh. Device and handle layers are separated by the thin buried silicon oxide layer that serves as an etch stop for both front and back side etches.

4. STRUCTURAL HIERARCHY FOR LARGE-AREA CAT GRATINGS

For application in an objective grating spectrometer with a large geometrical aperture gratings need to cover a large area, and grating support structures must be kept as small as possible to minimize x ray absorption. Free standing CAT gratings can be etched out of a microns-thin membrane, but such thin membranes need to be stiffened and supported in order to span larger areas. To that avail we employ a hierarchy of structural supports, starting with a $5 - 10 \mu\text{m}$ -period support mesh (Level 1 or L1 supports) that is integrated in the CAT grating layer and holds the CAT grating bars in place. This layer is etched from the device layer of an SOI wafer. The next level of supports is a hexagonal L2 mesh (hexagon diameter $\sim 0.5 - 2 \text{ mm}$), which we etch from the $\sim 0.5 \text{ mm}$ -thick handle layer of the SOI wafer. We refer to the resulting structure as a grating membrane. This membrane is then bonded to a machined frame (facet frame, L3 support) to form a grating facet of $\sim 10 - 50 \text{ cm}^2$ in area. Finally, many facets are assembled into a grating array that is held together by a grating array structure (GAS).

Wet etching in KOH with proper grating pattern alignment to the silicon $\langle 111 \rangle$ planes that are normal to the $\langle 110 \rangle$ surface provides almost atomically smooth grating bar sidewalls. However, inclined $\langle 111 \rangle$ planes lead to rapid undesired broadening of L1 supports with increasing etch depth.⁵ We have thus developed a deep reactive-ion etch (DRIE) process that enables us to simultaneously etch the CAT grating and L1 support patterns vertically into the device layer up to $6 \mu\text{m}$ in depth.^{12,26} Unfortunately the resulting sidewalls are rough and require subsequent polishing.

5. CAT GRATING FABRICATION PROCESS AND RECENT PROGRESS

Our CAT grating membrane fabrication process consists of the following steps: Beginning with a $\langle 110 \rangle$ SOI wafer (device layer thickness is the desired grating bar depth) we pattern the back (handle layer) and front (device layer) side. The front side thermal silicon oxide mask contains the CAT grating pattern, and the low-duty-cycle resist mask for the L1 support mesh runs on top of the oxide mask in the perpendicular direction. We then transfer the combined pattern vertically into the device layer until the DRIE stops on the buried oxide (BOX) layer. Due to the high thermal load from the DRIE process the wafer needs to be cooled from the back during etching. Cooling is even more important during the much more rapid and powerful back side etch and must take place through the front side. Thus, before proceeding to the back side etch, we fill and protect the grating with

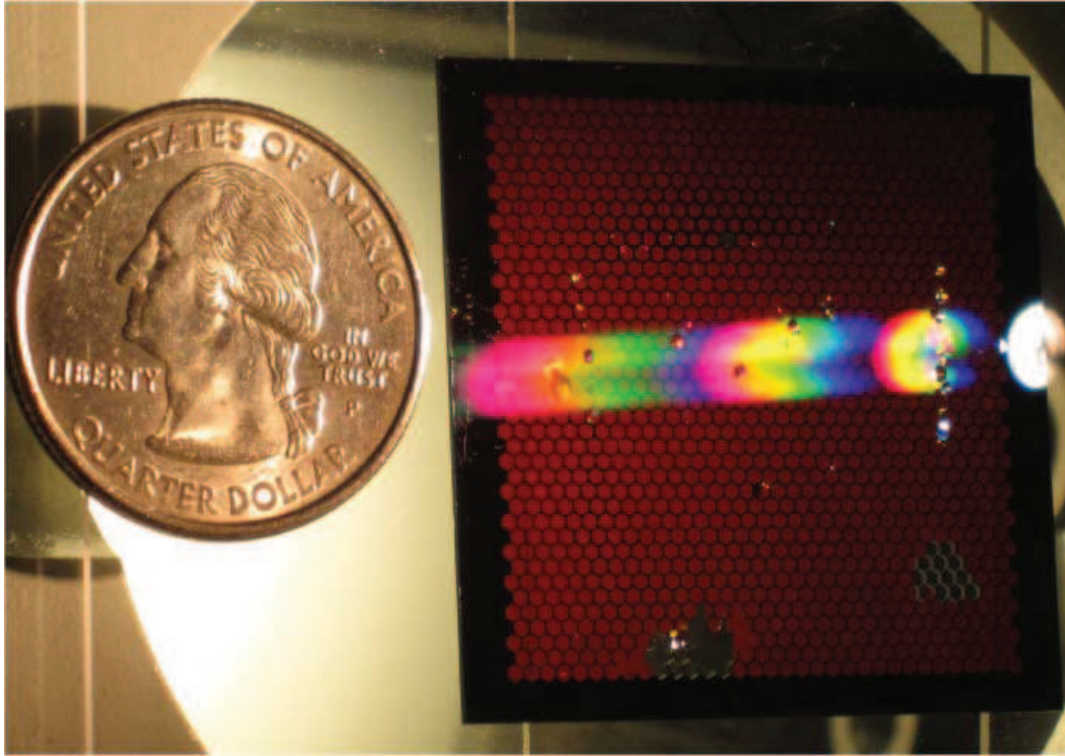


Figure 4. Grating membrane next to a U.S. quarter coin. Diffraction is due to the L1 support mesh. The hexagonal L2 mesh is visible due to back illumination. Most membrane defects were caused by mechanical interactions²⁷ (intentional tearing with tweezers and tape for cross sectional inspection, covering with silicon chips to mitigate etch non-uniformities).

resist and bond the front side to a carrier wafer. Bonding is followed by back side DRIE - again stopping on the BOX layer - and BOX removal in hydrofluoric acid. Next we separate the sample from the carrier wafer, clean out the protective resist from the CAT grating, and dry the sample in a critical-point dryer. Not surprisingly, each of these steps can be broken down into numerous sub-steps with their own yield and compatibility issues. In particular, the decision whether to etch the front or the back side first has tradeoffs that are difficult to predict before experimenting with both approaches. More detail about the final fabrication process can be found in other publications.^{12,27}

Previously²⁶ we have only shown successful fabrication results for individual features of the hierarchical facet structure, such as front side oxide masks on top of the device and BOX layers and the L2 mesh, or front side etch results on bulk silicon wafers, etc. Here we show for the first time results of complete membranes with a hexagonal L2 mesh spanning $31 \times 31 \text{ mm}^2$ that supports a 4 micron thick device layer from which L1 supports and CAT grating bars have been etched (see Fig. 4). Fig. 5 shows a back side view of the L2 mesh. Barely visible are the L1 supports that have been etched through from the front side. The zoomed-in view clearly shows the 5 micron-period L1 supports and the 200 nm-period CAT grating bars. In Fig. 6 we see a cross section view of the device layer from a different sample, showing again how CAT grating bars and L1 supports are etched straight through the device layer.

6. DISCUSSION, SUMMARY, AND OUTLOOK

We have demonstrated experimentally that it is possible to fabricate large-area CAT grating structures with a hierarchy of low-obscuration supports. As mentioned above, the CAT grating sidewalls resulting from the DRIE are too rough to blaze x rays efficiently. We therefore have begun to investigate wet KOH polishing of the sidewalls after DRIE. This requires precise alignment of the CAT grating pattern to the vertical $\langle 111 \rangle$ planes of the SOI device layer. Line edge roughness in the mask leads to rapid undercutting during the KOH

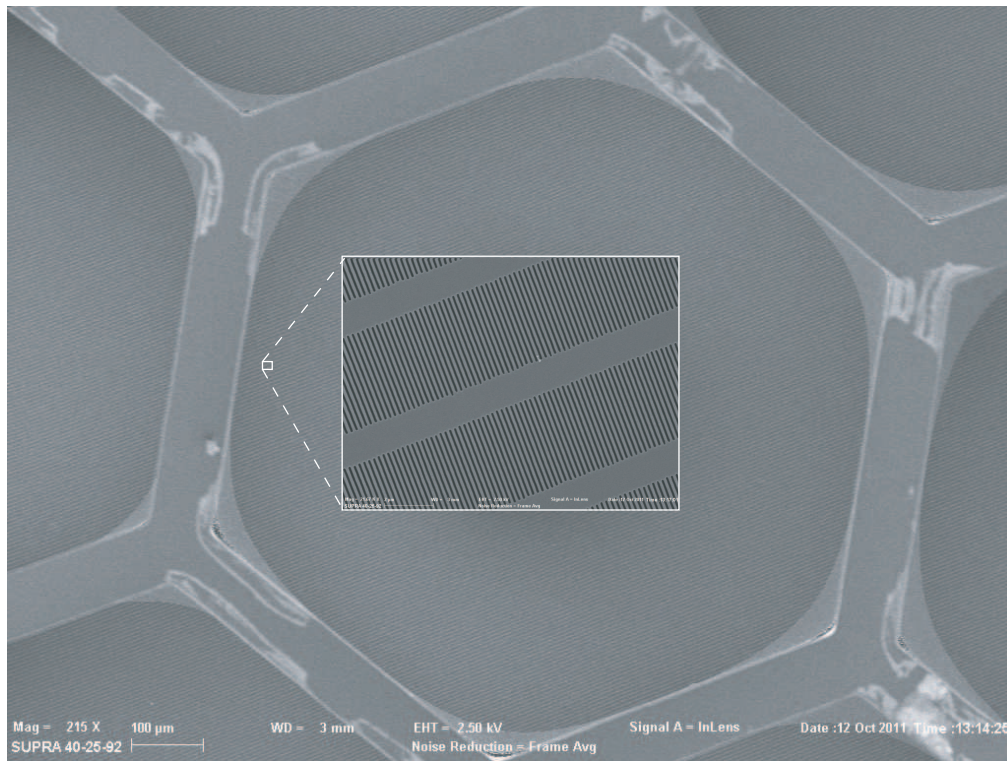


Figure 5. Scanning electron micrograph (SEM) of the back side of a grating membrane. The hexagon period is ~ 1 mm, and the L2 mesh lines are $\sim 100 \mu\text{m}$ wide. The insert shows a small area of the membrane back side at larger magnification.

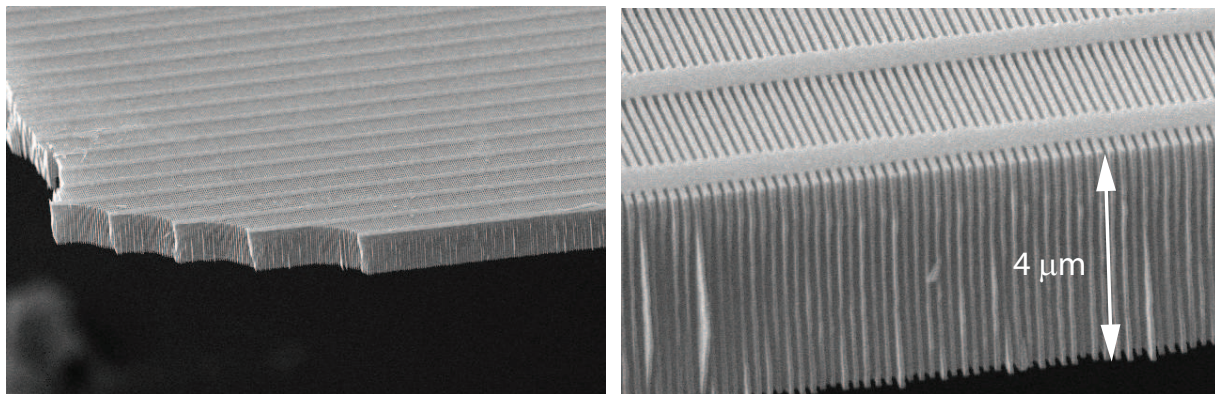


Figure 6. SEM of an etched device layer ripped out of a hexagonal cell for cross-sectional inspection. (Left) View of a torn membrane edge, showing the L1 support lines and CAT grating bar cross sections. (Right) Zoomed-in view of grating bar cross sections. “Wiggleness” in the lines is due to SEM vibrations.

etch and needs to be minimized.¹¹ The polishing step can potentially be added to the existing fabrication process at different points. We will explore the most sensible options. We are also in the process of bringing our scanning-beam interference lithography tool²⁸ back online after a major refurbishment. This tool is expected to improve our control of alignment and contrast during the CAT grating patterning process, which will reduce undercutting. We also plan to install a dedicated DRIE tool at MIT to optimize the DRIE process for deeper etches. Polished CAT gratings will undergo x-ray testing for efficiency and subsequently be integrated into a spectrometer bread board. We are developing in parallel models and test objects for the structural optimization of the L2 mesh and external flight frames.

ACKNOWLEDGMENTS

We gratefully acknowledge technical support from F. DiPiazza (Silicon Resources) and facilities support from the Nanostructures Laboratory and the Microsystems Technology Laboratories (both at MIT). This work was performed in part at the Lurie Nanofabrication Facility, a member of the National Nanotechnology Infrastructure Network, which is supported by the National Science Foundation. This work was supported by NASA grant NNX11AF30G.

REFERENCES

- [1] C. R. Canizares *et al.*, “The Chandra high-energy transmission grating: Design, fabrication, ground calibration, and 5 years in flight,” *PASP* **117**, 1144-1171 (2005).
- [2] J. W. den Herder *et al.*, “The reflection grating spectrometer on board XMM-Newton,” *Astr. & Astroph.* **365**, L7-L17 (2001).
- [3] R. K. Heilmann, M. Ahn, E. M. Gullikson, and M. L. Schattenburg, “Blazed high-efficiency x-ray diffraction via transmission through arrays of nanometer-scale mirrors,” *Opt. Express* **16**, 8658-8669 (2008).
- [4] R. K. Heilmann, M. Ahn, and M. L. Schattenburg, “Fabrication and performance of blazed transmission gratings for x-ray astronomy,” *Proc. SPIE* **7011**, 701106 (2008).
- [5] R. K. Heilmann, M. Ahn, A. Bruccoleri, C.-H. Chang, E. M. Gullikson, P. Mukherjee, and M. L. Schattenburg, “Diffraction efficiency of 200 nm period critical-angle transmission gratings in the soft x-ray and extreme ultraviolet wavelength bands,” *Appl. Opt.* **50**, 1364-1373 (2011).
- [6] R. K. Heilmann *et al.*, “Critical-angle transmission gratings for high resolution, large area soft x-ray spectroscopy,” Response to NASA solicitation NNH11ZDA018L, <http://pcos.gsfc.nasa.gov/studies/rfi/Heilmann-Ralf-RFINNH11ZDA018L.pdf> (2011).
- [7] K. Flanagan *et al.*, “Spectrometer concept and design for x-ray astronomy using a blazed transmission grating,” *Proc. SPIE* **6688**, 66880Y (2007).
- [8] R. K. Heilmann *et al.*, “Development of a critical-angle transmission grating spectrometer for the International X-Ray Observatory,” *Proc. SPIE* **7437**, 74370G (2009).
- [9] R. K. Heilmann *et al.*, “Critical-angle transmission grating spectrometer for high-resolution soft x-ray spectroscopy on the International X-Ray Observatory,” *Proc. SPIE* **7732**, 77321J (2010).
- [10] M. Ahn, R. K. Heilmann, and M. L. Schattenburg, “Fabrication of ultrahigh aspect ratio freestanding gratings on silicon-on-insulator wafers,” *J. Vac. Sci. Technol. B* **25**, 2593-2597 (2007).
- [11] M. Ahn, R. K. Heilmann, and M. L. Schattenburg, “Fabrication of 200 nm-period blazed transmission gratings on silicon-on-insulator wafers,” *J. Vac. Sci. Technol. B* **26**, 2179-2182 (2008).
- [12] P. Mukherjee, A. Bruccoleri, R. K. Heilmann, M. L. Schattenburg, A. F. Kaplan, and L. J. Guo, “Plasma etch fabrication of 60:1 aspect ratio silicon nanogratings on 200 nm pitch,” *J. Vac. Sci. Technol. B* **28**, C6P70-5 (2010).
- [13] “New Worlds, New Horizons in Astronomy and Astrophysics,” National Research Council, http://www.nap.edu/catalog.php?record_id=12951 (2010).
- [14] J. Bookbinder, “An overview of the IXO Observatory,” *Proc. SPIE* **7732**, 77321B (2010).
- [15] R. L. McEntaffer *et al.*, “Development of off-plane gratings for WHIMex and IXO,” *Proc. SPIE* **8147**, 81471K (2011).
- [16] K. Nandra, “Athena: The advanced telescope for high energy astrophysics,” these proceedings (2012).

- [17] J. A. Bookbinder *et al.*, “AXSIO - The Advanced X-ray Spectroscopic Imaging Observatory,” Response to NASA solicitation NNH11ZDA018L, <http://pcos.gsfc.nasa.gov/studies/rfi/Bookbinder-Jay-RFI-NNH11ZDA018L.pdf> (2011).
- [18] J. A. Bookbinder *et al.*, “The Advanced X-ray Spectroscopic Imaging Observatory (AXSIO),” these proceedings (2012).
- [19] M. W. Bautz *et al.*, “AEGIS - an astrophysics experiment for grating and imaging spectroscopy,” Response to NASA solicitation NNH11ZDA018L, <http://pcos.gsfc.nasa.gov/studies/rfi/Bautz-Marshall-RFINNH11ZDA018L.pdf> (2011).
- [20] J. E. Davis, M. W. Bautz, D. Dewey, R. K. Heilmann, J. C. Houck, D. P. Huenemoerder, H. L. Marshall, M. A. Nowak, and M. L. Schattenburg, “A ray-trace model for AEGIS,” these proceedings (2012).
- [21] M. W. Bautz *et al.*, “Concepts for high-performance soft x-ray grating spectroscopy in a moderate-scale mission,” these proceedings (2012).
- [22] A. Vikhlinin *et al.*, “SMART-X, square meter, arcsecond resolution x-ray telescope,” Response to NASA solicitation NNH11ZDA018L, <http://pcos.gsfc.nasa.gov/studies/rfi/Vikhlinin-Alexey-RFI.pdf>
- [23] A. Vikhlinin *et al.*, “SMART-X: A large-area, high-resolution x-ray observatory for the 2020’s,” these proceedings (2012).
- [24] W. C. Cash Jr., “X-ray optics 2: A technique for high-resolution spectroscopy,” *Appl. Opt.* **30**, 1749-1759 (1991).
- [25] R. L. Kelley *et al.*, “The high resolution microcalorimeter soft x-ray spectrometer for the Astro-H mission,” these proceedings (2012).
- [26] R. K. Heilmann, A. Bruccoleri, P. Mukherjee, J. Yam, and M. L. Schattenburg, “Fabrication update on critical-angle transmission gratings for soft x-ray grating spectrometers,” *Proc. SPIE* **8147**, 81471L (2011).
- [27] A. Bruccoleri, P. Mukherjee, R. K. Heilmann, J. Yam, and M. L. Schattenburg, “Fabrication of nano-scale, high throughput, high aspect-ratio freestanding gratings,” submitted to *J. Vac. Sci. Technol. B* (2012).
- [28] R. K. Heilmann, C. G. Chen, P. T. Konkola, and M. L. Schattenburg, “Dimensional metrology for nanometer-scale science and engineering: Towards sub-nanometer accurate encoders,” *Nanotechnology* **15**, S504 (2004).